iScience

CellPress
OPEN ACCESS

Article

CD6 deficiency impairs early immune response to bacterial sepsis

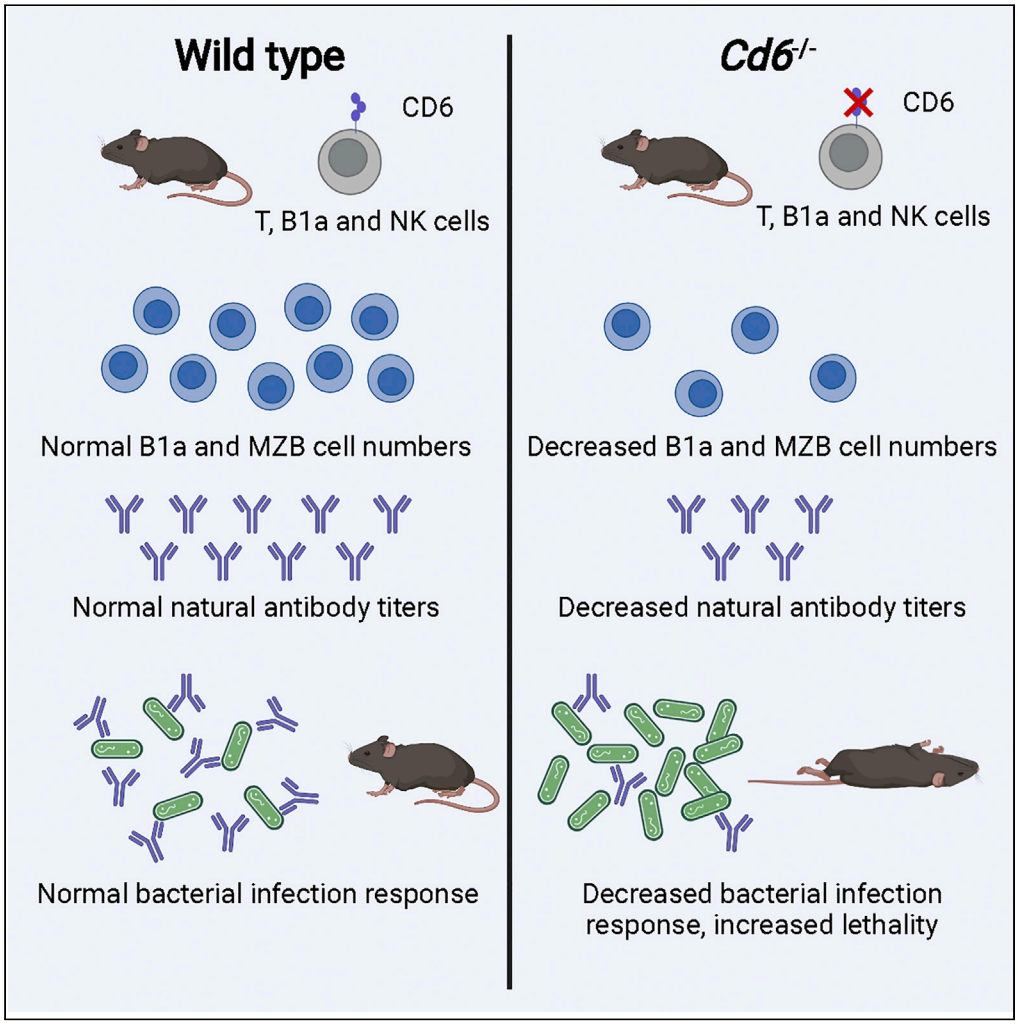

Cristina Català, María Velasco-de Andrés, Alejandra Leyton-Pereira, ..., Pablo Engel, Gustavo Mourglia-Ettlin, Francisco Lozano

flozano@clinic.cat

Highlights

CD6 is a nonredundant receptor in early immune response to sepsis

Cd6−/− mice show higher susceptibility to bacterial sepsis

Cd6−/− mice show lower B1a and MZB cell and natural polyreactive antibody levels

B cell and serum transfer restore susceptibility of *Cd6*−/− mice to bacterial sepsis

Català et al., iScience *25*, 105078
October 21, 2022
https://doi.org/10.1016/j.isci.2022.105078

iScience

CellPress
OPEN ACCESS

Article

CD6 deficiency impairs early immune response to bacterial sepsis

Cristina Català,[1] María Velasco-de Andrés,[1] Alejandra Leyton-Pereira,[1] Sergi Casadó-Llombart,[1] Manuel Sáez Moya,[5] Rebeca Gutiérrez-Cózar,[5] Joaquín García-Luna,[2] Marta Consuegra-Fernández,[1] Marcos Isamat,[3] Fernando Aranda,[4] Mario Martínez-Florensa,[1] Pablo Engel,[1,5] Gustavo Mourglia-Ettlin,[2] and Francisco Lozano[1,5,6,7,*]

SUMMARY

CD6 is a lymphocyte-specific scavenger receptor expressed on adaptive (T) and innate (B1a, NK) immune cells, which is involved in both fine-tuning of lymphocyte activation/differentiation and recognition of bacterial-associated molecular patterns (i.e., lipopolysaccharide). However, evidence on CD6's role in the physiological response to bacterial infection was missing. Our results show that induction of monobacterial and polymicrobial sepsis in *Cd6*$^{-/-}$ mice results in lower survival rates and increased bacterial loads and pro-inflammatory cytokine levels. Steady state analyses of *Cd6*$^{-/-}$ mice show decreased levels of natural polyreactive antibodies, concomitant with decreased cell counts of spleen B1a and marginal zone B cells. Adoptive transfer of wild-type B cells and mouse serum, as well as a polyreactive monoclonal antibody improve *Cd6*$^{-/-}$ mouse survival rates post-sepsis. These findings support a nonredundant role for CD6 in the early response against bacterial infection, through homeostatic expansion and functionality of innate-related immune cells.

INTRODUCTION

Bacterial sepsis is a devastating condition resulting from a dysregulated immune response to infection, leading to a sustained pro-inflammatory state and eventually, to organ dysfunction and death (Singer et al., 2016). This response is triggered by conserved and broadly distributed structures present on bacterial cell walls generically named microbial-associated molecular patterns (MAMPs) (Janeway and Medzhitov, 2002). Examples of bacterial MAMPs include the lipopolysaccharide (LPS) from Gram-negative strains, lipoteichoic acid (LTA) and peptidoglycan (PGN) from Gram-positive ones, and unmethylated CpG DNA islands. Bacterial MAMPs recognition by the host's immune system relies on the so-called pattern recognition receptors (PRRs), a series of nonpolymorphic, nonclonally distributed, and germ-line-encoded receptors from different structural protein families (Medzhitov, 2007), such as Toll-like receptors (TLRs), nucleotide oligomerization domain (NOD)-like receptors (NLRs), C-type lectin receptors (CLRs), absent in melanoma 2 (AIM2)-like receptors (ALRs), and scavenger receptors (SRs), among others (Li and Wu, 2021). These PRRs are broadly distributed among innate and adaptive immune cells, and exposure to their ligands activates the expression of inflammatory and immune response genes (Akira et al., 2006).

CD6 is a lymphoid-specific member of the SR class I group characterized by several conserved repeats of the scavenger receptor cysteine-rich (SRCR) domain (Taban et al., 2022). CD6 is expressed on adaptive (T) and innate (B1a, NK) immune cells and is involved in (1) fine-tuning of lymphocyte activation/differentiation and (2) recognition of MAMPs (Sarukhan et al., 2016). CD6 consists of three extracellular SRCR tandem domains, a transmembrane region and a cytoplasmic tail with Ser/Thr/Tyr residues responsive through phosphorylation to signaling effectors (Sarukhan et al., 2016). This allows CD6 to modulate the signals delivered by the T and B cell receptor complexes, to which it physically associates (Gimferrer et al., 2004; Gonçalves et al., 2018). Recent studies show that the TCR-inducible CD6 signalosome comprises both positive (SLP-76, ZAP70, VAV1) and negative (UBASH3A/STS-2) regulators of T cell activation, which account for the long-standing difficulties in classifying it as an inhibitory or stimulatory co-receptor (Mori et al., 2021).

The extracellular region of CD6 interacts with endogenous ligands such as CD166/ALCAM (for activated leukocyte cell adhesion molecule)—a broadly distributed cell adhesion molecule involved in T-APC

[1]Institut d'Investigacions Biomèdiques August Pi i Sunyer (IDIBAPS), Rosselló 149-153, 08036 Barcelona, Spain

[2]Área Inmunología, Facultad de Química/Facultad de Ciencias, DEPBIO/IQB, Universidad de la República, 11800 Montevideo, Uruguay

[3]Sepsia Therapeutics S.L., 08908 L'Hospitalet de Llobregat, Spain

[4]Center for Applied Medical Research (CIMA), University of Navarra, 31008 Pamplona, Spain

[5]Departament de Biomedicina, Facultat de Medicina, Universitat de Barcelona, 08036 Barcelona, Spain

[6]Servei d'Immunologia, Centre de Diagnòstic Biomèdic (CDB), Hospital Clínic de Barcelona, 08036 Barcelona, Spain

[7]Lead contact

*Correspondence: flozano@clinic.cat

https://doi.org/10.1016/j.isci.2022.105078

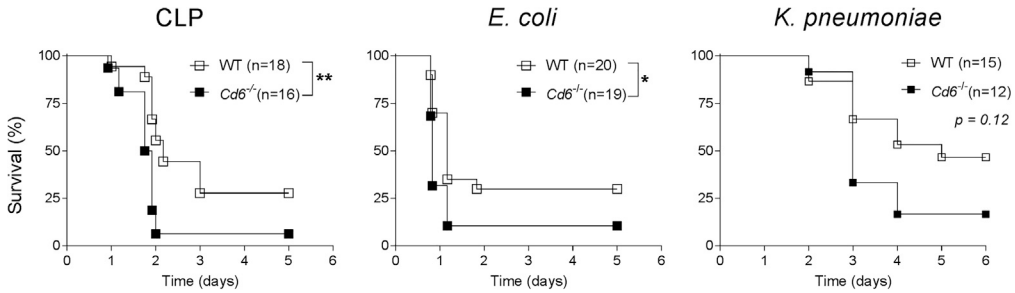

Figure 1. *Cd6*$^{-/-}$ mice show higher susceptibility to different experimental models of bacterial sepsis

WT and *Cd6*$^{-/-}$ mice were subjected to CLP-induced peritonitis (**left**), *E. coli*-induced peritonitis (9×10^6 CFU/mouse, *i.p.*) (**middle**) or *K. pneumoniae*-induced pneumonitis (9×10^8 CFU/mouse, *i.n.*) (**right**). Percent average of mouse survival is represented over time. *p < 0.05; **p < 0.01 (Gehan-Breslow-Wilcoxon test).

stabilization and leukocyte/lymphocyte extravasation (Bowen et al., 2000; Ferragut et al., 2021); CD318/CDCP-1 (for CUB Domain-Containing Protein 1) (Enyindah-Asonye et al., 2017a); and galectins 1 and 3 (Escoda-Ferran et al., 2014; Liu, 2005). The same extracellular region also subserves PRR functions by sensing and interacting with MAMPs of bacterial (LPS, LTA, PGN) origin (Martínez-Florensa et al., 2014; Sarrias et al., 2007). In addition, LPS binding to membrane-bound CD6 delivers MAPK pathway activation signals via Erk1/2 phosphorylation (Sarrias et al., 2007). Bacterial MAMPs recognition by CD6 maps to short peptide sequences (11-mer long) at each SRCR domain (Martínez-Florensa et al., 2018). Interestingly, infusion of either soluble CD6 protein or CD6-based peptides results in therapeutic effects in mouse models of monobacterial and polymicrobial sepsis (Martínez-Florensa et al., 2014, 2017, 2018). On this basis, we hypothesize that CD6$^+$ immune cells sense bacterial MAMPs and signal their functional status (Lenz, 2009; Sarrias et al., 2007), defining a physiological role for CD6 in the host's response to bacterial infection. We have investigated this role using CD6-deficient mice (*Cd6*$^{-/-}$) in different experimental models of sepsis.

RESULTS

CD6 deficiency confers susceptibility to bacterial sepsis

Upon induction of different models of monobacterial (*Escherichia coli*-induced peritonitis and *Klebsiella pneumoniae*-induced pneumonitis) and polymicrobial (cecal ligation and puncture [CLP]-induced peritonitis) sepsis, *Cd6*$^{-/-}$ mice from C57BL/6 background (Orta-Mascaró et al., 2016) showed lower survival rates compared with wild-type (WT) littermate controls (Figure 1). Further *in vivo* analyses of *Cd6*$^{-/-}$ mice after CLP-induced sepsis showed higher peritoneum and spleen bacterial loads (Figure 2A), and higher plasma and/or peritoneum pro-inflammatory cytokines (interleukin-6 [IL-6] and TNF-α) (Figure 2B), together with a trend to lower peritoneal neutrophil infiltration (Figure 2C). These results indicate that CD6 deficiency confers a nonspecific susceptibility to bacterial sepsis, which could result from impaired innate and/or adaptive immune responses.

Innate B cell subsets and natural polyreactive antibodies are decreased in CD6-deficient mice

In order to screen immune response in *Cd6*$^{-/-}$ mice, B cell populations were studied, as they have been previously linked to bacterial sepsis resolution (Boes et al., 1998; Kelly-Scumpia et al., 2011). B cell studies from steady state mice showed no differences between *Cd6*$^{-/-}$ and WT littermate controls regarding total peritoneal and spleen B cell numbers (Figure 3A left and 3B left). However, *Cd6*$^{-/-}$ mice showed lower spleen but not peritoneum B1a cell numbers (Figure 3A right and 3B middle), in agreement with previous data from *Cd6*$^{-/-}$ mice of different (DBA-1) genetic background (Enyindah-Asonye et al., 2017b). Moreover, numbers of marginal zone B (MZB) cells, a CD6-negative spleen B cell subpopulation also linked to innate immune functions (Palm and Kleinau, 2021), were also lower in our *Cd6*$^{-/-}$ mice compared with WT littermates (Figure 3B **right**).

Spleen B1a and MZB cells are considered the main source of natural polyreactive antibodies (NAbs), which in turn are known to play an important role in the innate immune response against bacterial infection (Aziz et al., 2015; Rohrbeck et al., 2021; Zhou et al., 2007). On this basis, *in vitro* and *in vivo* production of anti-dinitrophenol (DNP) antibodies—a surrogate for NAbs (Gunti et al., 2015)—was investigated in *Cd6*$^{-/-}$ mice of C57BL/6 background. Thus, *in vitro* stimulation of splenocytes from steady-state *Cd6*$^{-/-}$ and WT littermate mice with different LPS doses for 24 h showed lower anti-DNP IgM levels in the former case (Figure 4A), suggesting a lower sensitivity to LPS sensing. In addition, serum analyses showed lower

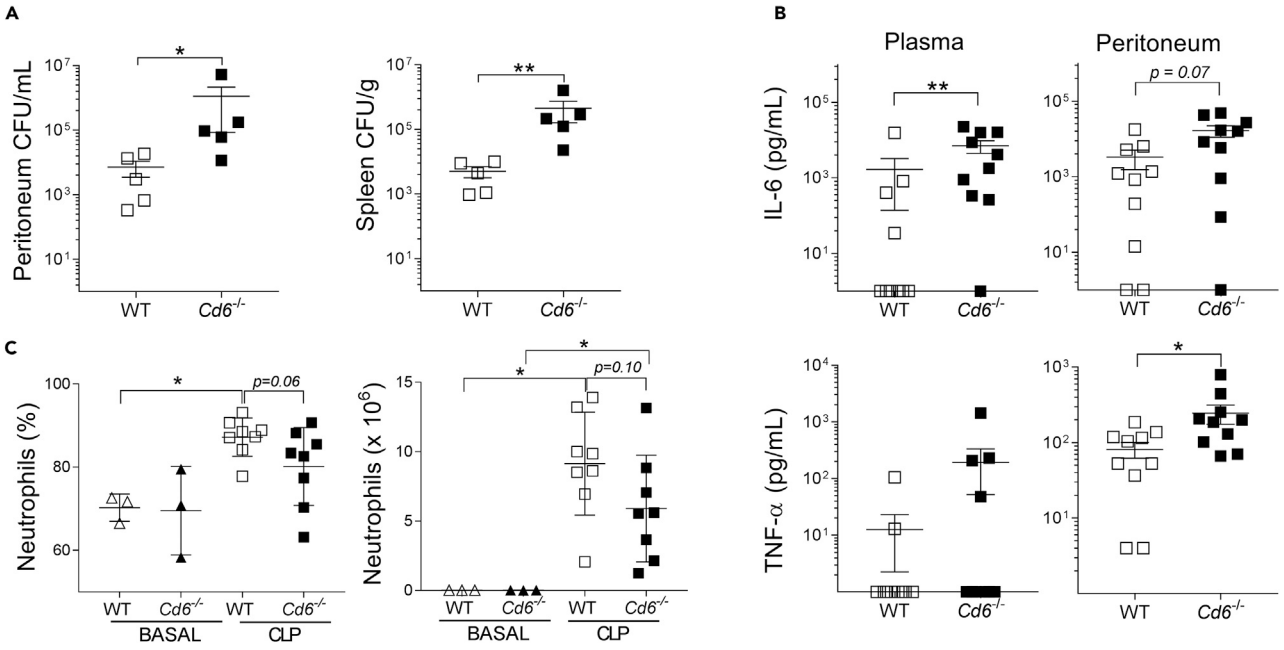

Figure 2. *Cd6*$^{-/-}$ mice show poor prognosis markers post-CLP induced sepsis

(A) Bacterial load post-CLP. Bacterial burden in peritoneum (**left**) and spleen (**right**) from WT and *Cd6*$^{-/-}$ mice was assessed at 24 h post-CLP induction. Data are expressed as mean ± SEM of CFU/g or CFU/mL. A representative experiment of 3 independently performed experiments is shown. *p < 0.05; **p < 0.01 (Mann-Whitney test).

(B) Cytokine levels post-CLP. Plasma and peritoneum IL-6 and tumor necrosis factor aloha (TNF-α) levels from WT and *Cd6*$^{-/-}$ mice were assessed by ELISA at 24 h post-CLP induction. Data are expressed as mean ± SEM. A representative experiment of 3 independently performed is shown. *p < 0.05; **p < 0.01 (Mann-Whitney test).

(C) Peritoneal neutrophil infiltration pre- and post-CLP. Percentage (**left**) and absolute number (**right**) of neutrophil (Gr1^{+}F4/80^{-}) in peritoneum from WT and *Cd6*$^{-/-}$ mice was assessed under basal conditions and 24 h post-CLP. A representative experiment of 3 independently performed is shown. *p < 0.05 (Mann-Whitney test).

levels of anti-DNP antibodies of different classes (immunoglobulin M [IgM] and IgA) and subclasses (IgG2b and IgG2c) for steady-state *Cd6*$^{-/-}$ mice compared with WT controls (Figure 4B). The latter result would again agree with similar findings in *Cd6*$^{-/-}$ mice from DBA-1 background, in which only total IgM polyreactive antibodies were found to be lowered (Enyindah-Asonye et al., 2017b).

Adoptive B cell and serum transfer improve sepsis-induced *Cd6*$^{-/-}$ mice survival

The involvement of B cells and NAbs in the increased susceptibility of *Cd6*$^{-/-}$ mice to bacterial infection was investigated by a series of adoptive cell and serum transfer experiments. First, adoptive transfer of negatively sorted spleen B cells the day before CLP induction improved *Cd6*$^{-/-}$ mice survival rates only when B cells were from WT but not from *Cd6*$^{-/-}$ mice (Figure 5A). Such protective effect may be attributable to B1a and MZB cells, as they are underrepresented in the spleen B cell pool from *Cd6*$^{-/-}$ mice (Figure 3B). As shown in Figure 5B, no protective effect was seen in CLP-induced sepsis survival of *Cd6*$^{-/-}$ mice upon prior transfer of wild-type T and NK cells. Next, amelioration of *Cd6*$^{-/-}$ mouse survival post-CLP induction was also observed upon transfer of pooled inactivated whole sera from WT but not from *Cd6*$^{-/-}$ mice (Figure 6A). Due to the complex composition of whole serum, such a protective effect cannot be unequivocally attributed to the NAbs fraction. So, additional transfer experiments were performed using a previously reported polyreactive mAb (H2h4-7-50) of the IgG2b subclass (Sáez Moya et al., 2021). As illustrated in Figures 6B–6D, H2h4-7-50 mAb transfer improved CLP-induced *Cd6*$^{-/-}$ mouse survival in a dose-dependent manner, together with a trend to reduced total peritoneum and spleen bacterial burdens and IL-6 systemic levels.

DISCUSSION

The results of the present work advocate for increased susceptibility of *Cd6*$^{-/-}$ mice to bacterial infection as supported from lower sepsis survival rates, lower bacterial clearance, higher pro-inflammatory cytokines, and lower peritoneal neutrophil infiltration. All these parameters are considered poor prognostic markers

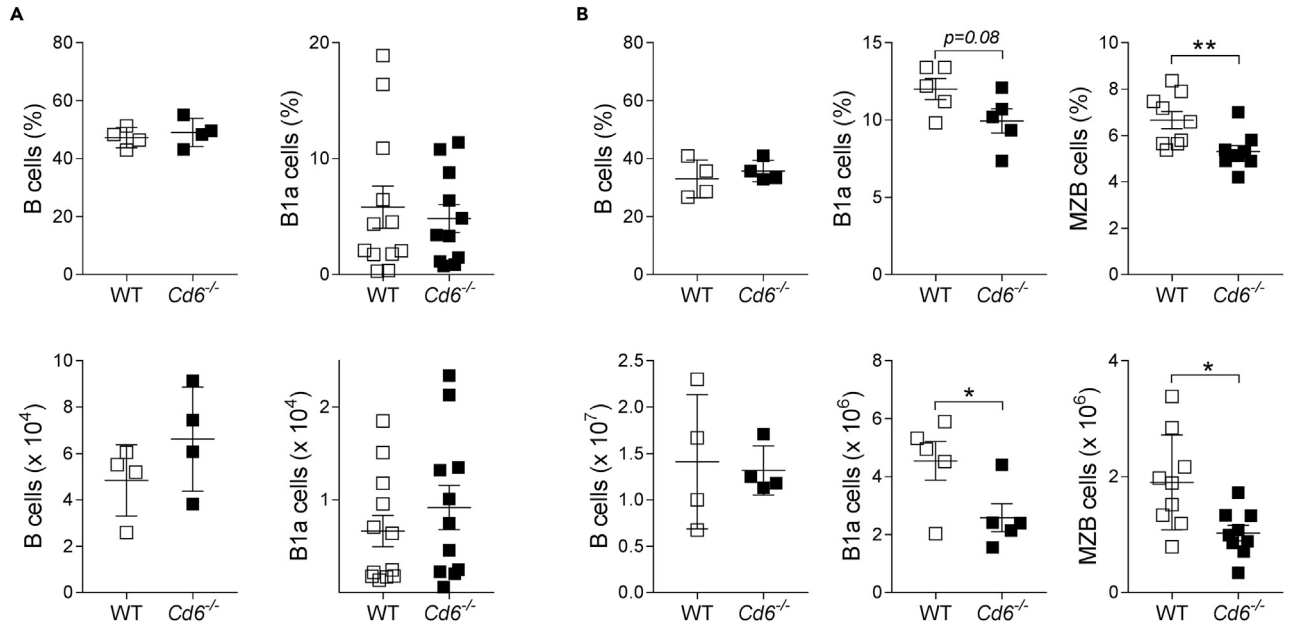

Figure 3. Steady state *Cd6*$^{-/-}$ mice show low spleen B1a and MZB cell levels

(A) Percentage and absolute numbers of peritoneal B ($CD19^+$) and B1a ($CD19^+CD11b+CD5^+$) cells as assessed by flow cytometry. Mean ± SEM is indicated. *$p < 0.05$ (Mann-Whitney test).

(B) Percentage and absolute numbers of spleen B ($CD19^+$), B1a ($CD19^+CD5^+$), and MZB ($B220^+CD21^+CD23^-$) cells as assessed by flow cytometry. Mean ± SEM is indicated. *$p < 0.05$; **$p < 0.01$ (Mann-Whitney test).

in experimental models of bacterial sepsis (Jin et al., 2017; Remick et al., 2002) and stand for a nonspecific susceptibility of *Cd6*$^{-/-}$ mice to bacterial infection, likely as a result of qualitative and/or quantitative defects in their innate and/or adaptive immune response. The fact that experimental bacterial sepsis models are acute (>50% mortality in 24 h to 72 h), with no time to mount effective adaptive immune responses, makes quite plausible the assumption of main innate immune response involvement. Nevertheless, available evidence also supports the involvement of T and B cells in the physiopathology of sepsis (Kasten et al., 2010; Kelly-Scumpia et al., 2011).

B cells constitute a heterogeneous cellular compartment with different functional and phenotypical properties (B1a, B1b, MZB, transitional and follicular B cells), which play pivotal roles in both innate and adaptive immune responses (Vaughan et al., 2011). The classical roles attributed to B cells during the immune response against infectious agents include production of antibodies and presentation of microbial antigens to T cells, as well as cytokine production upon activation by bacterial products (e.g., LPS). Work carried out in B-cell-deficient mice ($\mu MT^{-/-}$) showed that B cells constitute early innate immune response enhancers for bacterial sepsis (Kelly-Scumpia et al., 2011). Such mice showed increased susceptibility to CLP-induced sepsis, which was T-cell-independent and overcome when $\mu MT^{-/-}$ mice were transferred with B cells or whole normal (WT) mouse serum, as well as when treated with CXCL10, a type I interferon (IFN)-inducible chemokine. Further work demonstrated that those sepsis-protective effects could be assigned to the B1a cell subset (Aziz et al., 2017). Our B cell studies showed that *Cd6*$^{-/-}$ mice have lower levels of B1a and MZB cells, two cell subsets implicated in NAbs secretion. Indeed, the antibacterial activity of NAbs include binding to both Gram-negative and Gram-positive bacteria, inhibition of bacterial growth by lysis, enhancement of phagocytosis, and neutralization of the functional activity of endotoxin (Zhou et al., 2007). Pioneer work using mutant mice in which B cells do not secrete IgM (though still express surface IgM and IgD and undergo class switching) first demonstrated the importance of endogenous natural IgM in early defense against severe bacterial infections (Boes et al., 1998). Such mice showed increased susceptibility to CLP-induced sepsis associated to increased bacterial loads and serum levels of pro-inflammatory cytokines and decreased neutrophil recruitment. Moreover, resistance to CLP was restored when soluble IgM-deficient mice were reconstituted with polyclonal IgM from normal mouse sera.

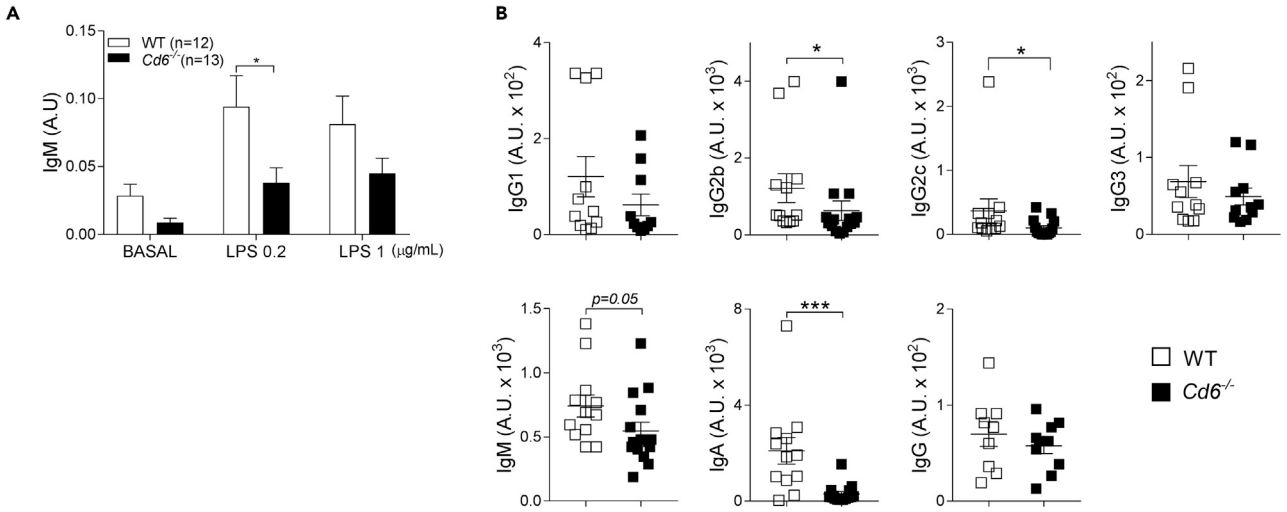

Figure 4. Steady state *Cd6*$^{-/-}$ mice show low *in vitro* and *in vivo* NAbs levels

(A) Splenocytes (2 × 10^5 cells) from steady state WT and *Cd6*$^{-/-}$ mice were stimulated *in vitro* for 24 h with different concentrations of LPS. Anti-DNP IgM levels in culture supernatants were assessed by ELISA. Data are expressed as mean ± SEM arbitrary units (A.U.). *p < 0.05 (two-way ANOVA, Sidak's multiple comparisons test).

(B) Serum anti-DNP IgM, IgG, IgG1, IgG2b, IgG2c, IgG3, and IgA levels from steady state mice were assessed by ELISA. Data are expressed as mean ± SEM A.U. *p < 0.05; **p < 0.01; ***p < 0.001 (Mann-Whitney test).

Importantly, our results show that *Cd6*$^{-/-}$ mice's decreased levels of NAbs involve not only IgM but also IgA and some IgG subclasses, which imply involvement of B cells able to undergo class-switch recombination events. NAbs of IgM class have long been associated not only with B1a cells (Baumgarth et al., 1999, 2000; Chou et al., 2009; Thurnheer et al., 2003) but also with MZB cells (Palm and Kleinau, 2021; Rohrbeck et al., 2021). Nevertheless, it has been recently claimed that most serum IgM in resting mice is produced by a discrete subset of bone marrow resident CD5$^-$ IgM plasma cells originated from fetal-lineage progenitors residing in the peritoneal cavity (neither B1a nor B1b) (Reynolds et al., 2015). Regarding NAbs of IgA class, it is considered that Peyer's patches would be the main place of production independently of germinal centers and through both T-dependent (TD) and T-independent (TI) pathways (Bunker et al., 2017; Shimoda et al., 1999) and that B1 cells would not be relevant contributors (Thurnheer et al., 2003). Altogether, the deficient production of NAbs in *Cd6*$^{-/-}$ mice would not involve a single B cell subset. However, adoptive B cell and serum transfer improved sepsis-induced *Cd6*$^{-/-}$ mice survival, indicating a nonredundant role of such components in *Cd6*$^{-/-}$ mice's immune response to sepsis.

Taken together, our results support quantitative and/or qualitative B1a and MZB cell defects and decreased availability of NAbs as a cause behind *Cd6*$^{-/-}$ mouse' increased susceptibility to bacterial infection. To the best of our knowledge, the only B cell subset expressing CD6 are B1a cells once they move from the peritoneal cavity to the spleen (Enyindah-Asonye et al., 2017b). CD6 expression gain for B1a cell function remains unexplored. Recent signalosome studies indicate that CD6 may recruit intracellular signal effectors in T cells (Mori et al., 2021), which may also be the case for B cells. Thus, CD6 may behave as a co-stimulatory or inhibitory receptor depending on the T/B cell stimulation conditions and/or the cell differentiation program. If the activating function dominates, CD6 deficiency may result in lower B1a homeostatic proliferation and antibody production. On the contrary, when the inhibitory function dominates, CD6-deficient B1a cells can be overactivated and undergo activation-induced cell death (AICD), also resulting in lower cell numbers and antibody production. In this regard, impaired B1a cell self-renewal has been reported to cause reduced B1a cell population in *Cd6*$^{-/-}$ mice (Enyindah-Asonye et al., 2017b).

Higher activation in B cells has been associated to worse sepsis outcome in humans (Monserrat et al., 2013) and mice (Nolan et al., 2009). Analysis of peritoneum and spleen total B cells after CLP-induced sepsis showed a higher induction of the co-stimulatory CD80 and CD86 receptors for *Cd6*$^{-/-}$ mice compared with WT controls (Figures S1A and S1B). This finding would be indicative of overactivation of *Cd6*$^{-/-}$ B cells 24 h post-CLP. As mentioned earlier, such overactivation in the minor B cell subset constitutively expressing CD6 (i.e., B1a cells) could still be the consequence of absent CD6-mediated inhibitory signals. However, the assessment

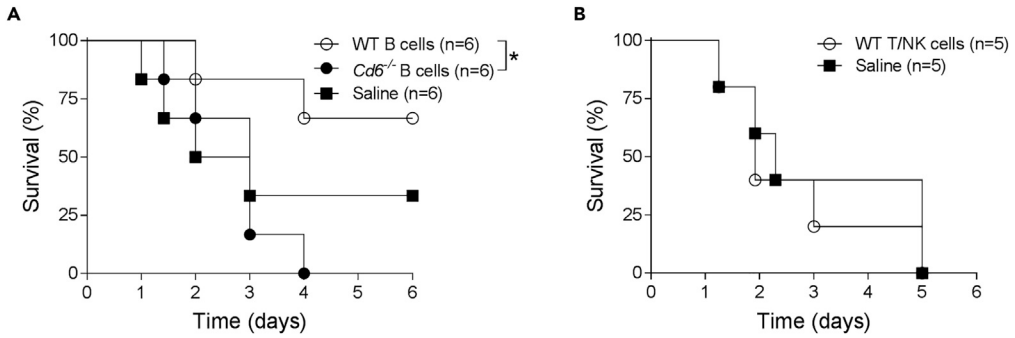

Figure 5. Adoptive WT B cell transfer improves *Cd6*$^{-/-}$ mice survival to CLP-induced sepsis

(A) *Cd6*$^{-/-}$ mice were *i.p.* pre-treated overnight with 10^7 cells/mouse of negatively sorted (GR1$^-$CD11c$^-$CD3$^-$NK1.1$^-$) spleen B cells from WT or *Cd6*$^{-/-}$ mice, before CLP induction. Percent average of mouse survival is represented over time. *p < 0.05 (Gehan-Breslow-Wilcoxon test).

(B) *Cd6*$^{-/-}$ mice were *i.p.* pre-treated overnight with negatively sorted (GR1$^-$CD11c$^-$CD19$^-$B220$^-$) spleen T and NK cells (10^7 cells/mouse) from WT mice, before CLP induction. Percent average of mouse survival is represented over time. *p < 0.05; **p < 0.01 (Gehan-Breslow-Wilcoxon test).

of apoptotic (Annexin V$^+$ and 7-AAD$^+$) B cells from spleen and peritoneum of WT and *Cd6*$^{-/-}$ mice before and 24 h post-CLP induction did not reveal significant differences (Figure S1C). This would indicate that overactivation of *Cd6*$^{-/-}$ B cells does not drive them to increased AICD induction. In case of the major B cell subset not constitutively expressing CD6 (B2), overactivation could result from other indirect causes such as a defective function of cells with regulatory/suppressive activity. Indeed, previous work from our group shows that steady state *Cd6*$^{-/-}$ mice already present higher frequencies of regulatory T (Treg) cells with decreased suppressive activity (Consuegra-Fernández et al., 2017; Orta-Mascaró et al., 2016). *Ex vivo* cell analyses showed that spleens from *Cd6*$^{-/-}$ mice post-CLP-induced sepsis also undergo higher Treg cell induction, associated to lower induction of CD69 surface expression, a maker correlating with Treg suppressive function (Yu et al., 2018) (Figure S2). Recent evidence shows that Treg cells, in addition to regulating adaptive immune responses, also regulate the function of innate immune cells such as macrophages, dendritic cells, and neutrophils (Okeke and Uzonna, 2019). As an example, it has been shown that Treg cells induce neutrophil recruitment through the production of CXCL8 (Himmel et al., 2011). Though the role of Tregs in immune response to infection is controversial, our findings would be compatible with the view of Tregs being important for successful elimination of bacteria and prevention of bacteria-induced hyperinflammation (i.e., systemic inflammatory response syndrome, SIRS) (Bosmann and Ward, 2013).

There are also claims that T cells act as early mediators in host response to sepsis (Kasten et al., 2010). During sepsis, T cell apoptosis occurs and attenuates the innate immune response through direct and indirect effects on macrophages and neutrophils, resulting in decreased control of bacterial infection and worsened outcomes. In a scenario of dysfunctional *Cd6*$^{-/-}$ Treg cells, excessive AICD of T cells might occur, which would be detrimental for bacterial sepsis survival. Accordingly, increased T cell AICD phenomena have been previously reported in *Cd6*$^{-/-}$ mice following their polyclonal activation (by co-crosslinking of CD3 and CD28) (Li et al., 2017).

In conclusion, our studies in *Cd6*$^{-/-}$ mice support an important role for the lymphocyte surface receptor CD6 during early/innate response against bacterial infections. The data point to CD6 expression as a key factor in the homeostatic expansion and functionality of relative small, though functionally relevant, B (B1a and MZB) and T (Treg) cell subsets. The consequences of such defects, either alone or in coordination, drive to a defective NAbs production and, consequently, to the loss of an important humoral element of the innate immune system. In this regard, clinical studies showed that the IgM levels are lower among nonsurvivor patients undergoing sepsis (Giamarellos-Bourboulis et al., 2013). Therefore, intravenous administration of IgM-enriched immunoglobulins has been tried in different clinical trials, exhibiting still unclear benefits probably due to the sepsis status of the patient at the moment of the infusion (Cui et al., 2019).

Limitations of the study

This manuscript addresses the function of CD6 in a bacterial sepsis context. However, it remains to be tested whether such susceptibility is general and extendable to other infectious agents (e.g., viruses, fungi, or

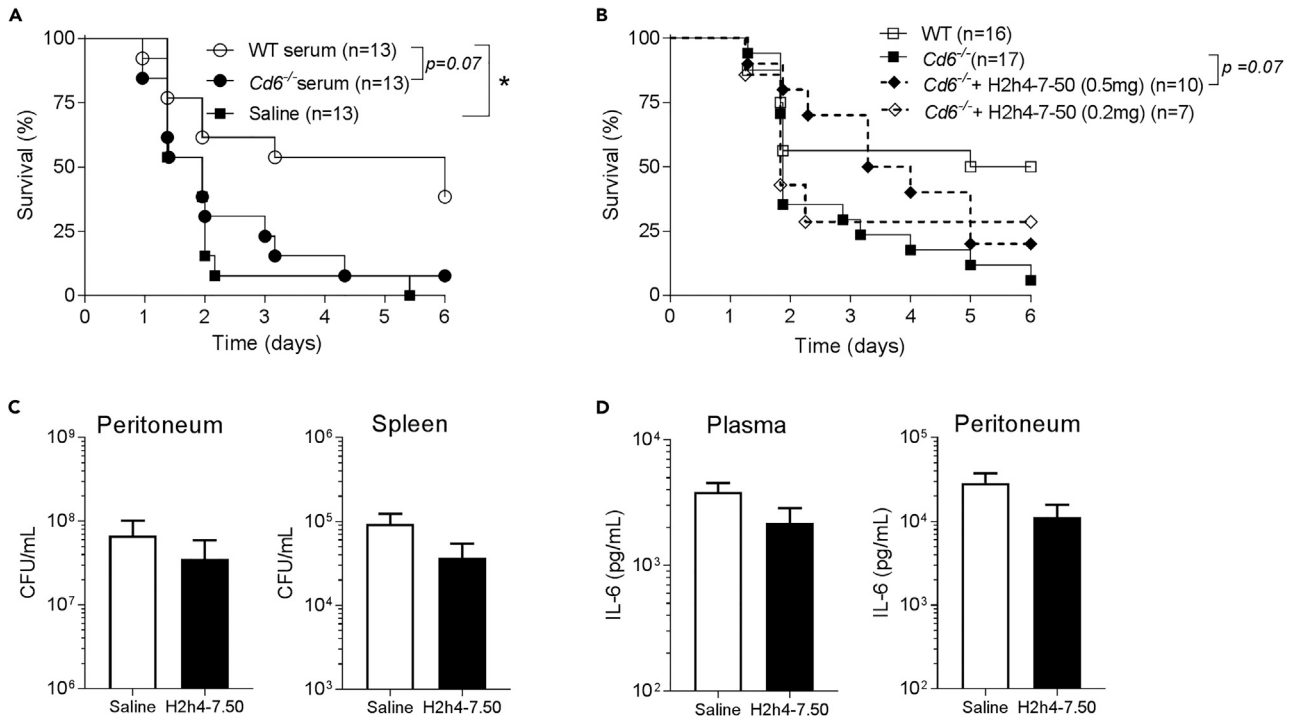

Figure 6. Adoptive antibody transfer improves *Cd6*$^{-/-}$ mice survival to CLP-induced sepsis

(A) *Cd6*$^{-/-}$ mice were *i.p.* pre-treated overnight with inactivated pooled whole sera (400 μL/mouse, diluted 1:2 in PBS) from *Cd6*$^{-/-}$ or WT mice before CLP induction. Percent average of mouse survival is represented over time. *p < 0.05 (Gehan-Breslow-Wilcoxon test).

(B) *Cd6*$^{-/-}$ mice were *i.p.* pre-treated overnight with saline or different doses of the H2h4-7-50 mAb (0.2 or 0.5 mg/mouse) before CLP-induction. Percent average of mouse survival is represented over time. *p < 0.05 (Gehan-Breslow-Wilcoxon test).

(C) Bacterial burden in peritoneum and spleen from saline (n = 5) or H2h4-7-50 mAb (n = 5) pre-treated *Cd6*$^{-/-}$ mice was determined at 24 h post-CLP induction. Data are expressed as mean ± SEM CFU/mL or CFU/g. *p < 0.05 (Mann-Whitney test).

(D) Plasma and peritoneum IL-6 levels from the same mice as in (C) were monitored at 24 h post-CLP induction by ELISA. Data expressed as mean ± SEM. *p < 0.05 (Mann-Whitney test).

parasites). Indeed, interaction of CD6 with certain viral, fungal, and parasitic structures has been reported (Velasco-de Andrés et al., Cells 2020). Moreover, B1a and MZB cell deficiency found in *Cd6*$^{-/-}$ mice could also be deeply studied in order to find the molecular and functional causes behind this deficiency. This approach will be partly addressed by studying how CD6-deficiency impacts the development of different B cell subsets (either CD6-positive or -negative), because low but significant surface CD6 expression levels have been reported in early (CD34^{+} rho123$^{med/lo}$) progenitors in bone marrow (Cortés et al., 1999).

STAR★METHODS

Detailed methods are provided in the online version of this paper and include the following:

- KEY RESOURCES TABLE
- RESOURCE AVAILABILITY
  - Lead contact
  - Materials availability
  - Data and code availability
- EXPERIMENTAL MODEL AND SUBJECT DETAILS
- METHOD DETAILS
  - *In vivo* infection models
  - *Ex vivo* phenotypical cell analyses
  - Polyreactive natural antibody measurements
- QUANTIFICATION AND STATISTICAL ANALYSIS

SUPPLEMENTAL INFORMATION

Supplemental information can be found online at https://doi.org/10.1016/j.isci.2022.105078.

ACKNOWLEDGMENTS

The work was supported by Spanish Ministerio de Economía y Competitividad (MINECO; SAF2016-80535-R) and Ministerio de Ciencia e Innovación (MCIN/AEI/10.13039/501100011033; PID2019-106658RB-I00), co-financed by European Development Regional Fund "A way to achieve Europe" ERDF, and Agència de Gestió d'Ajuts Universitaris i de Recerca (AGAUR; 2017/SGR/1582) from Generalitat de Catalunya. CC, MV-dA, SC-L, and AL-P are recipients of fellowships from Spanish Ministerio de Economía y Competitividad (MINECO; BES-2017-082107 and BES-2014-069237), Ministerio de Educación, Cultura y Deporte (FPU15/02897), and Chilean Agencia Nacional de Investigación y Desarrollo (ANID; 2018-72190154), respectively. Graphical abstract was created with BioRender.com.

AUTHOR CONTRIBUTIONS

F.L., M.I., F.A., MM-F, GM-E, and P.E. conceptualized and designed the studies. C.C., MV-dA, AL-P, SC-L, MS-M, RG-C, JG-L, MC-F., F.A., and MM-F performed mouse studies. C.C., M.I., and F.L. wrote the original draft. All authors read, critically revised, and approved the final version of the manuscript.

DECLARATION OF INTEREST

F.L. and M.I. are founders and ad-honorem scientific advisors of Sepsia Therapeutics S.L. F.L. is the inventor of patents WO2008119851A1, WO2018091679A1, and WO2019/175261A1. The rest of the authors have no additional financial interests.

Received: March 22, 2022
Revised: July 15, 2022
Accepted: August 31, 2022
Published: October 21, 2022

REFERENCES

Akira, S., Uematsu, S., and Takeuchi, O. (2006). Pathogen recognition and innate immunity. Cell *124*, 783–801.

Aziz, M., Holodick, N.E., Rothstein, T.L., and Wang, P. (2015). The role of B-1 cells in inflammation. Immunol. Res. *63*, 153–166.

Aziz, M., Holodick, N.E., Rothstein, T.L., and Wang, P. (2017). B-1a cells protect mice from sepsis: critical role of CREB. J. Immunol. *199*, 750–760.

Baumgarth, N., Herman, O.C., Jager, G.C., Brown, L., Herzenberg, L.A., and Herzenberg, L.A. (1999). Innate and acquired humoral immunities to influenza virus are mediated by distinct arms of the immune system. Proc. Natl. Acad. Sci. USA *96*, 2250–2255.

Baumgarth, N., Herman, O.C., Jager, G.C., Brown, L.E., Herzenberg, L.A., and Chen, J. (2000). B-1 and B-2 cell-derived immunoglobulin M antibodies are nonredundant components of the protective response to influenza virus infection. J. Exp. Med. *192*, 271–280.

Boes, M., Prodeus, A.P., Schmidt, T., Carroll, M.C., and Chen, J. (1998). A critical role of natural immunoglobulin M in immediate defense against systemic bacterial infection. J. Exp. Med. *188*, 2381–2386.

Bosmann, M., and Ward, P.A. (2013). The inflammatory response in sepsis. Trends Immunol. *34*, 129–136.

Bowen, M.A., Aruffo, A.A., and Bajorath, J. (2000). Cell surface receptors and their ligands: in vitro analysis of CD6-CD166 interactions. Proteins *40*, 420–428.

Bunker, J.J., Erickson, S.A., Flynn, T.M., Henry, C., Koval, J.C., Meisel, M., Jabri, B., Antonopoulos, D.A., Wilson, P.C., and Bendelac, A. (2017). Natural polyreactive IgA antibodies coat the intestinal microbiota. Science *358*, eaan6619.

Chou, M.Y., Fogelstrand, L., Hartvigsen, K., Hansen, L.F., Woelkers, D., Shaw, P.X., Choi, J., Perkmann, T., Bäckhed, F., Miller, Y.I., et al. (2009). Oxidation-specific epitopes are dominant targets of innate natural antibodies in mice and humans. J. Clin. Invest. *119*, 1335–1349.

Consuegra-Fernández, M., Martínez-Florensa, M., Aranda, F., de Salort, J., Armiger-Borràs, N., Lozano, T., Casares, N., Lasarte, J.J., Engel, P., and Lozano, F. (2017). Relevance of CD6-mediated interactions in the regulation of peripheral T-cell responses and tolerance. Front. Immunol. *8*, 594.

Cortés, F., Deschaseaux, F., Uchida, N., Labastie, M.C., Friera, A.M., He, D., Charbord, P., and Péault, B. (1999). HCA, an immunoglobulin-like adhesion molecule present on the earliest human hematopoietic precursor cells, is also expressed by stromal cells in blood-forming tissues. Blood *93*, 826–837.

Cui, J., Wei, X., Lv, H., Li, Y., Li, P., Chen, Z., and Liu, G. (2019). The clinical efficacy of intravenous IgM-enriched immunoglobulin (pentaglobin) in sepsis or septic shock: a meta-analysis with trial sequential analysis. Ann. Intensive Care *9*, 27.

Enyindah-Asonye, G., Li, Y., Ruth, J.H., Spassov, D.S., Hebron, K.E., Zijlstra, A., Moasser, M.M., Wang, B., Singer, N.G., Cui, H., et al. (2017a). CD318 is a ligand for CD6. Proc. Natl. Acad. Sci. USA *114*, E6912–E6921.

Enyindah-Asonye, G., Li, Y., Xin, W., Singer, N.G., Gupta, N., Fung, J., and Lin, F. (2017b). CD6 receptor regulates intestinal ischemia/reperfusion-induced injury by modulating natural IgM-producing B1a cell self-renewal. J. Biol. Chem. *292*, 661–671.

Escoda-Ferran, C., Carrasco, E., Caballero-Baños, M., Miró-Julià, C., Martínez-Florensa, M., Consuegra-Fernández, M., Martínez, V.G., Liu, F.T., and Lozano, F. (2014). Modulation of CD6 function through interaction with Galectin-1 and -3. FEBS Lett. *588*, 2805–2813.

Ferragut, F., Vachetta, V.S., Troncoso, M.F., Rabinovich, G.A., and Elola, M.T. (2021). ALCAM/CD166: a pleiotropic mediator of cell adhesion, stemness and cancer progression. Cytokine Growth Factor Rev. *61*, 27–37.

Giamarellos-Bourboulis, E.J., Apostolidou, E., Lada, M., Perdios, I., Gatselis, N.K., Tsangaris, I., Georgitsi, M., Bristianou, M., Kanni, T., Sereti, K., et al. (2013). Kinetics of circulating immunoglobulin M in sepsis: relationship with final outcome. Crit. Care *17*, R247.

Gimferrer, I., Calvo, M., Mittelbrunn, M., Farnós, M., Sarrias, M.R., Enrich, C., Vives, J., Sánchez-Madrid, F., and Lozano, F. (2004). Relevance of CD6-mediated interactions in T cell activation and proliferation. J. Immunol. *173*, 2262–2270.

Gonçalves, C.M., Henriques, S.N., Santos, R.F., and Carmo, A.M. (2018). CD6, a rheostat-type signalosome that tunes T cell activation. Front. Immunol. *9*, 2994.

Gunti, S., Messer, R.J., Xu, C., Yan, M., Coleman, W.G., Peterson, K.E., Hasenkrug, K.J., and Notkins, A.L. (2015). Stimulation of Toll-Like Receptors profoundly influences the titer of polyreactive antibodies in the circulation. Sci. Rep. *5*, 15066–15068.

Himmel, M.E., Crome, S.Q., Ivison, S., Piccirillo, C., Steiner, T.S., and Levings, M.K. (2011). Human CD4+ FOXP3+ regulatory T cells produce CXCL8 and recruit neutrophils. Eur. J. Immunol. *41*, 306–312.

Janeway, C.A., and Medzhitov, R. (2002). Innate immune recognition. Annu. Rev. Immunol. *20*, 197–216.

Jin, L., Batra, S., and Jeyaseelan, S. (2017). Deletion of Nlrp3 augments survival during polymicrobial sepsis by decreasing autophagy and enhancing phagocytosis. J. Immunol. *198*, 1253–1262.

Kasten, K.R., Tschöp, J., Adediran, S.G., Hildeman, D.A., and Caldwell, C.C. (2010). T cells are potent early mediators of the host response to sepsis. Shock *34*, 327–336.

Kelly-Scumpia, K.M., Scumpia, P.O., Weinstein, J.S., Delano, M.J., Cuenca, A.G., Nacionales, D.C., Wynn, J.L., Lee, P.Y., Kumagai, Y., Efron, P.A., et al. (2011). B cells enhance early innate immune responses during bacterial sepsis. J. Exp. Med. *208*, 1673–1682.

Lenz, L.L. (2009). CD5 sweetens lymphocyte responses. Proc. Natl. Acad. Sci. USA *106*, 1303–1304.

Li, D., and Wu, M. (2021). Pattern recognition receptors in health and diseases. Signal Transduct. Target. Ther. *61*, 291–324.

Li, Y., Singer, N.G., Whitbred, J., Bowen, M.A., Fox, D.A., and Lin, F. (2017). CD6 as a potential target for treating multiple sclerosis. Proc. Natl. Acad. Sci. USA *114*, 2687–2692.

Liu, F.T. (2005). Regulatory roles of Galectins in the immune response. Int. Arch. Allergy Immunol. *136*, 385–400.

Martínez-Florensa, M., Català, C., Velasco-de Andrés, M., Cañadas, O., Fraile-Ágreda, V., Casadó-Llombart, S., Armiger-Borràs, N., Consuegra-Fernández, M., Casals, C., and Lozano, F. (2018). Conserved bacterial-binding peptides of the scavenger-like human lymphocyte receptor CD6 protect from mouse experimental sepsis. Front. Immunol. *9*, 627.

Martínez-Florensa, M., Consuegra-Fernández, M., Aranda, F., Armiger-Borràs, N., Di Scala, M., Carrasco, E., Pachón, J., Vila, J., González-Aseguinolaza, G., and Lozano, F. (2017). Protective effects of human and mouse soluble scavenger-like CD6 lymphocyte receptor in a lethal model of polymicrobial sepsis. Antimicrob. Agents Chemother. *61*. e01391-16.

Martínez-Florensa, M., Consuegra-Fernández, M., Martínez, V.G., Cañadas, O., Armiger-Borràs, N., Bonet-Roselló, L., Farrán, A., Vila, J., Casals, C., and Lozano, F. (2014). Targeting of key pathogenic factors from gram-positive bacteria by the soluble ectodomain of the scavenger-like lymphocyte receptor CD6. J. Infect. Dis. *209*, 1077–1086.

Medzhitov, R. (2007). Recognition of microorganisms and activation of the immune response. Nature *449*, 819–826.

Monserrat, J., de Pablo, R., Diaz-Martín, D., Rodríguez-Zapata, M., de la Hera, A., Prieto, A., and Alvarez-Mon, M. (2013). Early alterations of B cells in patients with septic shock. Crit. Care *17*, R105–R110.

Mori, D., Grégoire, C., Voisinne, G., Celis-Gutierrez, J., Aussel, R., Girard, L., Camus, M., Marcellin, M., Argenty, J., Burlet-Schiltz, O., et al. (2021). The T cell CD6 receptor operates a multitask signalosome with opposite functions in T cell activation. J. Exp. Med. *218*. e20201011.

Nolan, A., Kobayashi, H., Naveed, B., Kelly, A., Hoshino, Y., Hoshino, S., Karulf, M.R., Rom, W.N., Weiden, M.D., and Gold, J.A. (2009). Differential role for CD80 and CD86 in the regulation of the innate immune response in murine polymicrobial sepsis. PLoS One *4*, e6600.

Okeke, E.B., and Uzonna, J.E. (2019). The pivotal role of regulatory T cells in the regulation of innate immune cells. Front. Immunol. *10*, 680.

Orta-Mascaró, M., Consuegra-Fernández, M., Carreras, E., Roncagalli, R., Carreras-Sureda, A., Alvarez, P., Girard, L., Simões, I., Martínez-Florensa, M., Aranda, F., et al. (2016). CD6 modulates thymocyte selection and peripheral T cell homeostasis. J. Exp. Med. *213*, 1387–1397.

Palm, A.K.E., and Kleinau, S. (2021). Marginal zone B cells: from housekeeping function to autoimmunity? J. Autoimmun. *119*, 102627.

Remick, D.G., Bolgos, G.R., Siddiqui, J., Shin, J., and Nemzek, J.A. (2002). Six at six: interleukin-6 measured 6 h after the initiation of sepsis predicts mortality over 3 days. Shock *17*, 463–467.

Reynolds, A.E., Kuraoka, M., and Kelsoe, G. (2015). Natural IgM is produced by CD5- plasma cells that occupy a distinct survival niche in bone marrow. J. Immunol. *194*, 231–242.

Rittirsch, D., Huber-Lang, M.S., Flierl, M.A., and Ward, P.A. (2008). Immunodesign of experimental sepsis by cecal ligation and puncture. Nat. Protoc. *4*, 31–36.

Rohrbeck, L., Adori, M., Wang, S., He, C., Tibbitt, C.A., Chernyshev, M., Sirel, M., Ribacke, U., Murrell, B., Bohlooly-Y, M., et al. (2021). GPR43 regulates marginal zone B-cell responses to foreign and endogenous antigens. Immunol. Cell Biol. *99*, 234–243.

Sáez Moya, M., Gutiérrez-Cózar, R., Puñet-Ortiz, J., Rodríguez de la Concepción, M.L., Blanco, J., Carrillo, J., and Engel, P. (2021). Autoimmune B cell repertoire in a mouse model of sjögren's syndrome. Front. Immunol. *12*.

Sarrias, M.R., Farnós, M., Mota, R., Sánchez-Barbero, F., Ibáñez, A., Gimferrer, I., Vera, J., Fenutría, R., Casals, C., Yélamos, J., and Lozano, F. (2007). CD6 binds to pathogen-associated molecular patterns and protects from LPS-induced septic shock. Proc. Natl. Acad. Sci. USA *104*, 11724–11729.

Sarukhan, A., Martinez-Florensa, M., Escoda-Ferran, C., Carrasco, E., Carreras, E., and Lozano, F. (2016). Pattern recognition by CD6: a scavenger-like lymphocyte receptor. Curr. Drug Targets *17*, 640–650.

Shimoda, M., Inoue, Y., Azuma, N., and Kanno, C. (1999). Natural polyreactive immunoglobulin A antibodies produced in mouse Peyer's patches. Immunology *97*, 9–17.

Singer, M., Deutschman, C.S., Seymour, C.W., Shankar-Hari, M., Annane, D., Bauer, M., Bellomo, R., Bernard, G.R., Chiche, J.D., Coopersmith, C.M., et al. (2016). The third international consensus definitions for sepsis and septic shock (Sepsis-3). JAMA *315*, 801–810.

Taban, Q., Mumtaz, P.T., Masoodi, K.Z., Haq, E., and Ahmad, S.M. (2022). Scavenger receptors in host defense: from functional aspects to mode of action. Cell Commun. Signal. *20*, 2–17.

Thurnheer, M.C., Zuercher, A.W., Cebra, J.J., and Bos, N.A. (2003). B1 cells contribute to serum IgM, but not to intestinal IgA, production in gnotobiotic Ig allotype chimeric mice. J. Immunol. *170*, 4564–4571.

Vaughan, A.T., Roghanian, A., and Cragg, M.S. (2011). B cells–masters of the immunoverse. Int. J. Biochem. Cell Biol. *43*, 280–285.

Velasco-de Andrés, M., Casadó-Llombart, S., Català, C., Leyton-Pereira, A., Lozano, F., Aranda, F., Soluble, C.D.5, and CD6. (2020). Lymphocytic class I scavenger receptors as immunotherapeutic agents. Cells *9*, 2589. https://doi.org/10.3390/cells9122589.

Yu, L., Yang, F., Zhang, F., Guo, D., Li, L., Wang, X., Liang, T., Wang, J., Cai, Z., and Jin, H. (2018). CD69 enhances immunosuppressive function of regulatory T-cells and attenuates colitis by prompting IL-10 production. Cell Death Dis. *9*, 905.

Zhou, Z.H., Zhang, Y., Hu, Y.F., Wahl, L.M., Cisar, J.O., and Notkins, A.L. (2007). The broad antibacterial activity of the natural antibody repertoire is due to polyreactive antibodies. Cell Host Microbe *1*, 51–61.

STAR★METHODS

KEY RESOURCES TABLE

REAGENT or RESOURCE	SOURCE	IDENTIFIER
Antibodies		
FITC Anti-Mouse F4/80 Antigen (BM8.1)	Tonbo Biosciences	Cat# 35-4801, RRID:AB_2621714
APC Anti-Mouse Ly-6G (Gr-1) (RB6-8C5)	Tonbo Biosciences	Cat# 20–5931, RRID:AB_2621610
PE Anti-Human/Mouse CD45R (B220) (RA3-6B2) Antibody	Tonbo Biosciences	Cat# 50–0452, RRID:AB_2621764
APC anti-mouse CD80	BioLegend	Cat# 104714, RRID:AB_313135
PE Ms CD86 CF594 GL1 50ug	BD Biosciences	Cat# 567592, RRID:AB_2916657
VioletFluor 450 Anti-Mouse CD4 (RM4-5)	Tonbo Biosciences	Cat# 75–0042, RRID:AB_2621928
PerCP-Cyanine 5.5 Anti-Mouse CD25 (PC61.5)	Tonbo Biosciences	Cat# 65–0251, RRID:AB_2621889
PE anti-Human/Mouse Foxp3 (3G3)	Tonbo Biosciences	Cat# 50–5773, RRID:AB_2621797
APC anti-mouse CD69 (H1.2F3)	BioLegend	Cat# 104514, RRID:AB_492843
APC anti-mouse CD11b (M1/70)	eBioscience	Cat# 17-0112-82, RRID:AB_469343
PerCP-Cy5.5 anti-mouse CD5 (53–7.3)	BioLegend	Cat# 100623, RRID: AB_2563432
FITC CD21/CD35 (B3B4)	BD Biosciences	Cat# 553818, RRID:AB_395070
PE anti-mouse CD23 PE (7G6)	BD Biosciences	Cat# 553139, RRID:AB_394654
PE anti-mouse CD6 (OX-129)	BioLegend	Cat# 146404, RRID:AB_2562753
Violet Fluor anti-mouse CD11c (N418)	eBioscience	Cat# 48-0114-82, RRID:AB_1548654
PerCP Cy5.5 anti-mouse CD3 (145-2C11)	Tonbo	Cat# 65-0031, RRID:AB_2621872
PE anti-mouse NK1.1 (PK136)	BD Pharmingen™	Cat# 557391, RRID:AB_396674
Purified anti-mouse CD16/CD32 (2.4G2)	Tonbo	Cat# 70–0161, RRID:AB_2621487
HRP-conjugated anti-mouse IgM	Sigma-Aldrich	Cat# A8786, RRID:AB_258413
HRP-conjugated anti-mouse IgG	Sigma-Aldrich	Cat# A3673, RRID:AB_258099
Goat Anti-Mouse IgA-HRP	SouthernBiotech	Cat# 1040–05, RRID:AB_2714213
PECy7 anti-mouse CD19 (1D3)	Tonbo	Cat# 60–0193, RRID:AB_2621840
Biotin-SP-AffiniPure Goat Anti-Mouse IgG, Fc_ Subclass 1	Jackson Immunoresearch	Cat# 115-065-205, RRID:AB_2338571
Biotin-SP-AffiniPure Goat Anti-Mouse IgG, Fc_ Subclass 2b	Jackson Immunoresearch	Cat# 115-065-207, RRID:AB_2338573
Biotin-SP-AffiniPure Goat Anti-Mouse IgG, Fc_ Subclass 2c	Jackson Immunoresearch	Cat# 115-065-208, RRID:AB_2338574
Biotin-SP-AffiniPure Goat Anti-Mouse IgG, Fc_ Subclass 3	Jackson Immunoresearch	Cat# 115-065-209, RRID:AB_2338575
Affinity-purified polyreactive H2h4-7-50 (IgG2b) mAb	(Sáez Moya et al., 2021)	N/A
Bacterial and virus strains		
Klebsiella pneumoniae	ATCC	ATCC 13883
Escherichia coli	ATCC	ATCC 25922
Chemicals, peptides, and recombinant proteins		
Collagenase D	Roche	11088866001
DNase I	Roche	10104159001
RBC lysis buffer	eBioscience	00-4333-57
Anesketin (ketamine)	Dechra Veterinary Products SLU	N/A
Xylazine	Rompun, Bayer	N/A
Streptavidin-POD conjugate	Roche	11089153001
DNP-BSA	Biotools	D-5050-10
TMB Substrate Reagent Set	BD Biosciences	555214

(*Continued on next page*)

Continued

REAGENT or RESOURCE	SOURCE	IDENTIFIER
Critical commercial assays		
Mouse IL-6 ELISA OptEIA set	BD Biosciences	555240
TNF-α ELISA OptEIA set	BD Biosciences	558534
APC Annexin V Apoptosis Detection Kit with 7-AAD	Biolegend	640930
Experimental models: Organisms/strains		
Mouse: CD6KO in C57BL6N background	KOMP	$Cd6^{tm1(KOMP)Wtsi}$
Software and algorithms		
Gen 5	BioTek Instruments Inc.	N/A
FlowJo software	Tree Star, USA	N/A
GraphPad Prism 7	GraphPad Software	N/A
BioRender	BioRender	N/A

RESOURCE AVAILABILITY

Lead contact

Further information and requests for resources and reagents should be directed to and will be fulfilled by the lead contact Francisco Lozano (flozano@clinic.cat).

Materials availability

This study did not generate new unique reagents.

Data and code availability

Flow cytometry data reported in this paper will be shared by the lead contact upon request.

All raw data reported in this paper will be shared by the lead contact upon request.

This paper does not report original code.

Any additional information required to reanalyze the data reported in this paper is available from the lead contact upon request.

EXPERIMENTAL MODEL AND SUBJECT DETAILS

CD6-deficient mice (*Cd6−/−*) were generated in C57BL/6N background through the Mouse Biology Program (University of California, Davis, Davis, CA) using targeting vector DPGS00142_B_G12 from the trans-NIH Knock-Out Mouse Project (KOMP), and obtained from the KOMP repository (Orta-Mascaró et al., 2016). *Cd6−/−* and wild-type littermate (WT) mice were housed at the animal facilities of the Facultat de Medicina from the Universitat de Barcelona and their $CD6^{-}$negative/positive phenotype was monitored by flow cytometry analysis using PE-conjugated rat anti-mouse CD6 mAb (OX-129, Biolegend). Eight- to twelve-week-old male mice were used in all experiments. Experimental procedures were approved by the Animal Experimentation Ethical Committee from Universitat de Barcelona (ref. 255/17).

METHOD DETAILS

In vivo infection models

Cecal ligation and puncture (CLP) was used as a model of polymicrobial peritonitis-induced sepsis (Rittirsch et al., 2008). Briefly, mice were anesthetised via *i.p.* with ketamine (100 mg/kg; Anesketin, Dechra Veterinary Products SLU) and xylazine (10 mg/kg; Rompun, Bayer). The lower half of the abdomen was shaved and sterilized with ethanol and 1-cm incision was done. The cecum was externalized and the distal 50% or 75% (mid- or high-grade mortality, respectively) was ligated using silicone coated braided silk 3–0 (Covidien). Cecal material was released by one 'through and through' puncture with a 21-gauge needle and a drop of faecal matter was exuded before reinstating the cecum into the peritoneal cavity and suturing the muscle and skin with TC16 26mm needle silk 3–0 (06100, Laboratorio Aragó, S.L.). Closed suture was

cleaned with povidone-iodine. Mice were then *s.c.* administered with saline (0.5 mL) and buprenorphine (0.05 mg/kg/12 h) for hydration and analgesia purposes post-surgery.

Escherichia coli–induced peritonitis and *Klebsiella pneumoniae*-induced pneumonitis were used as models of monobacterial sepsis. Briefly, bacteria were grown in Luria Bertoni (LB) liquid cultures at 37°C under horizontal shaking at 180 rpm, centrifuged and suspended in saline to desired concentration. Mice were then infected with *E. coli* (9 × 106 CFU/mouse, *i.p.*; ATCC 25922) or *K. pneumoniae* (9 × 108 CFU/mouse, *i.n.*; ATCC 13883) and survival was monitored over time. Buprenorphine (0.05 mg/kg/12 h, *s.c.*) was administered for 3 days after infection.

For adoptive B and T plus NK cell transfer experiments, spleens from steady state *Cd6*$^{-/-}$ and WT littermate mice were homogenized. Splenocytes were suspended in 4 mL of 1× RBC lysis buffer (eBioscience) for 4 min at RT. After washing twice with PBS, cell pellets were suspended in PBS plus 10% FBS and pooled. Total B or NK and T cells were then negatively sorted in FACS Aria II and FACS Aria Sorp BD cytometers from IDIBAPS Flow cytometry platform, upon staining with the following fluorescent-labeled mAb mix for B cells sorting: GR-1-APC (RB6-8C5, Tonbo), CD11c-Violet Fluor (N418, eBioscience), CD3-PerCP-Cy5.5 (145-2C11, Tonbo) and NK1.1-PE (PK136, BD). For T and NK cells sorting, the mAb mix selected was: GR-1-APC (RB6-8C5, Tonbo), CD11c-Violet Fluor (N418, eBioscience), CD19-PECy7 (1D3, Tonbo) and CD45R/B220-Violet Fluor (RA3-6B2, Tonbo). Sorted WT and *Cd6*$^{-/-}$ B cells (96% purity) were collected, suspended in sterile saline and *i.p.* injected (10^7 cells/mouse) to *Cd6*$^{-/-}$ mice 15 h before CLP-induction. A control group of *Cd6*$^{-/-}$ mice was also *i.p.* injected with the same volume of vehicle. For T and NK transfer only WT cells were sorted (94% purity) and injected in the same conditions ad for B cell transfer experiment.

For serum transfer experiments, whole blood samples from steady state *Cd6*$^{-/-}$ and WT littermate mice were obtained by cardiac puncture and allowed to clot at RT. Then, samples were centrifuged (10 min at 2000 rcf) for serum isolation and pooling, and further complement inactivation by incubation at 56 C for 30 min. Inactivated pooled sera were diluted 1:2 in PBS (400 μL final volume/mouse) and injected *i.p.* 15 h before CLP-induction. In parallel experiments, affinity-purified polyreactive H2h4-7-50 (IgG2b) mAb (Sáez Moya et al., 2021) was also injected (0.2 or 0.5 mg/mouse, *i.p.*) 15 h before CLP-induction.

In all cases, survival was monitored over time. In some cases, mice were euthanized at 24 h post-CLP induction for organ samplings. Bacterial load measurements in peritoneal lavages and spleen homogenates were conducted by plating serial diluted samples (in sterile PBS) on LB agar, and incubated overnight at 37°C. Viable bacterial counts were expressed as CFU/mL or CFU/mg. IL-6 and TNF-α cytokine levels from plasma or peritoneal lavage samples were monitored by ELISA using OptEIA sets (BD Biosciences; catalogs no. 555240 and 558534, respectively) and following manufacturer's instructions. Absorbance (450 nm and 570 nm) was read using Epoch spectrophotometer (Biotek).

Ex vivo phenotypical cell analyses

Peritoneum cells from mice euthanized before and 24 h after CLP-induction were obtained by centrifugation (5 min at 1500 rpm) of peritoneal lavages. Cell pellets were suspended in 1 mL of 1× RBC lysis buffer (eBioscience) and incubated for 4 min at RT. After two PBS washings, cells were suspended in PBS plus 2% FBS for total cell counting using 0.4% Trypan Blue (SV30084.01, VWR). Spleens from mice euthanized before and 24 h after CLP-induction were aseptically removed and incubated for 20 min at 37°C in 3 mL of PBS containing collagenase D (1 mg/mL; Roche 11088866001) and DNase I (0.1 mg/mL; Roche 10104159001). Following disaggregation through 40 μm cell strainers with a syringe plunger, cells were washed with 10 mL of PBS. After discarding the supernatant, cells were incubated at RT for 4 min with 4 mL of RBC lysis buffer. Upon two PBS washings, cells were suspended in PBS plus 2% FBS for total cell counting using 0.4% Trypan Blue. Then, 106 cells/well were plated into 96-well plates and incubated for 15 min at RT in blocking solution (PBS plus 2% FBS and anti-mouse CD16/CD32; Fc Shield, clone 2.4G2, Tonbo Bioscience) for flow cytometry analyses. Mixes of mAbs were prepared in 2% FBS-PBS solution and 50 μL of each mix was added to the cells. Fluorescent-labeled mAbs used were: F4/80-FITC (BM8.1, Tonbo), GR-1-allophycocyanin (APC) (RB6-8C5, Tonbo), CD45R/B220-Violet Fluor (RA3-6B2, Tonbo), CD80-APC (16–10A1, Biolegend), CD86-PE (GL1, BD Pharmaginen), CD3-PerCP-Cy5.5 (145-2C11, Tonbo), CD4-Violet Fluor (75–0042, Tonbo), CD25-Peridinin Chlorophyll Protein-Cyanine5.5 (PerCP-Cy5.5) (65–0251, Tonbo), FoxP3-PE (3G3, Tonbo), CD69-APC (104514, Biolegend), CD11b-APC (M1/70, eBioscience), CD5-PerCP-Cy5.5 (53–7.3, Biolegend), CD21/CD35-FITC (B3B4, BD) and CD23-PE (7G6, BD). Cell samples

were incubated for 20 min at 4°C in dark, and then centrifuged at 1800 rpm, washed twice with PBS and suspended in fixing solution (PBS plus 1% paraformaldehyde). For apoptosis analysis APC Annexin V Apoptosis Detection Kit with 7-AAD (Biolegend, 640930) was used following manufacturer's instructions. Labeled cells were analyzed with a BD FACSCanto II flow cytometer (Becton Dickinson, US) and mean fluorescence intensity (MFI) data analyzed using FlowJo software (Tree Star, USA).

Polyreactive natural antibody measurements

For *in vitro* studies, spleens from steady state *Cd6-/-* and WT mice were aseptically isolated and processed as explained above. Cells were counted and adjusted to the desired concentration in RPMI 1640 medium plus L-glutamine (R8758–6X500ML; Sigma & Aldrich), FBS (10%), 2-Mercaptoethanol (50μM; Merck), penicillin (100 U/mL; 6191309, Lab EBN) and streptomycin (100 μg/mL; 624569, Lab Normon). 2 × 105cells/well were plated in U-bottomed 96-well plates (Biofil). Cells were stimulated with LPS (0.2 or 1 μg/mL) for 24 h.

Supernatants from *in vitro* studies and serum samples from *Cd6-/-* and WT steady state mice were serially diluted and plated into 96-well plates previously coated with dinitrophenol (DNP)-BSA (5 μg/mL; Biotools) overnight at 4°C and blocked with 1% BSA in PBS. After overnight incubation, plate-bound DNP-reactive IgM, IgG and IgA antibodies were developed by using HRP-conjugated anti-mouse Ig antibodies (Sigma A8786, A3673 and Southern Biotech 1040–05, respectively). Plate-bound DNP-reactive IgG1, IgG2b, IgG2c and IgG3 antibodies were developed by using biotin-labeled antibodies (Jackson Immunoresearch 115-065-205, 207, 208 and 209, respectively) plus streptavidin-POD conjugate (Roche 11089153001). Wellplates were developed using TMB Substrate Reagent Set (BD, 555214), and 2N H2SO4 was added to stop the reaction. Absorbance (450 nm and 570 nm) was read using Epoch spectrophotometer (Biotek).

QUANTIFICATION AND STATISTICAL ANALYSIS

GraphPad Prism 7 (GraphPad Software) was used to design graphs and for statistical comparisons. *p values $\leq$0.05 were considered statistically significant.